

# Theoretical Study To Explain How Chirality Is Stored and Evolves throughout the Radical Cascade Rearrangement of Enyne-allenes

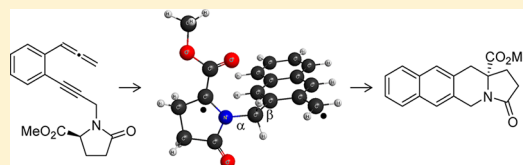
Anouk Gaudel-Siri,<sup>\*,†</sup> Damien Campolo,<sup>†</sup> Shovan Mondal,<sup>‡</sup> Malek Nechab,<sup>†</sup> Didier Siri,<sup>†</sup> and Michèle P. Bertrand<sup>†</sup>

<sup>†</sup>Aix-Marseille Université, CNRS, Institut de Chimie Radicalaire (UMR-7273), 13397 Marseille Cedex 20, France

<sup>‡</sup>Department of Chemistry, Visva Bharati University, Santiniketan, Birbhum, West Bengal 731235, India

## S Supporting Information

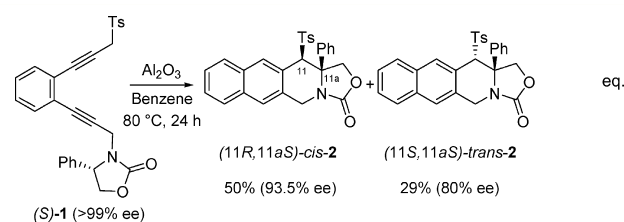
**ABSTRACT:** This article reports a theoretical study to explain how the intrinsic property of chirality is retained throughout the radical cascade rearrangement of an enantiopure chiral enyne-allene (bearing one stereogenic center) selected as a model for this family of reactions. Calculations at the MRPT2/6-31G(d)//CASSCF(10,10)/6-31G(d) level of theory were used to determine the entire reaction pathway which includes singlet state diradicals and closed-shell species. The cascade process involves three elementary steps, i.e., by chronological order: Myers–Saito cycloaromatization (M-S), intramolecular hydrogen atom transfer (HAT), and recombination of the resulting biradical. The enantiospecificity of the reaction results from a double transmission of the stereochemical information, from the original center to an axis and eventually from this axis to the final center. The first two steps lead to a transient diradical intermediate which retains the chirality via the conversion of the original static chirogenic element into a dynamic one, i.e., a center into an axis. The only available routes to the final closed-shell tetracyclic product imply rotations around two  $\sigma$  bonds ( $\sigma(\text{C}-\text{C})$  and  $\sigma(\text{C}-\text{N})$ , bonds  $\beta$  and  $\alpha$  respectively). The theoretical calculations confirmed that the formation of the enantiomerically pure product proceeds via the nonracemizing rotation around the  $\sigma(\text{C}-\text{C})$  pivot. They ruled out any rotation around the second  $\sigma(\text{C}-\text{N})$  pivot. The high level of configurational memory in this rearrangement relies on the steric impediment to the rotation around the C–N bond in the chiral native conformation of the diradical intermediate produced from tandem M-S/1,5-HAT.



## INTRODUCTION

The discovery of the powerful antitumor properties of enediyne-containing natural products<sup>1</sup> has stimulated innovative research in multidisciplinary fields. The biological activity of these compounds is related to their aptitude to rearrange into highly reactive diradicals,<sup>2,3</sup> capable of abstracting hydrogen atoms from DNA strands, which induces DNA cleavage and eventually cell death. Even though an impressive volume of literature data has been devoted to the cycloaromatization processes responsible for these properties, an ever sustained activity attests to the impact of these reactions in fields as diverse as biology, medicinal chemistry, and materials science.<sup>4,5</sup> In a recent review, Kraka et al. pointed out how much the enediyne reactivity has also impacted computational methodologies.<sup>6</sup>

We have recently investigated chirality transfer<sup>7</sup> in the cascade rearrangement of enediynes bearing a suitably located stereogenic center.<sup>8</sup> A first series of results was obtained from enediynes such as **1**, where the enyne-allene intermediate was generated in situ via base-catalyzed 1,3-proton shift (eq 1).<sup>8a,b</sup> These reactions were shown to proceed with a high level of retention of configuration at the original stereogenic center. However, due to the absence of control of the allene configuration in this procedure and to the creation of two stereocenters in the final product of which only one was controlled, the reaction led to a mixture of diastereomers as exemplified in eq.

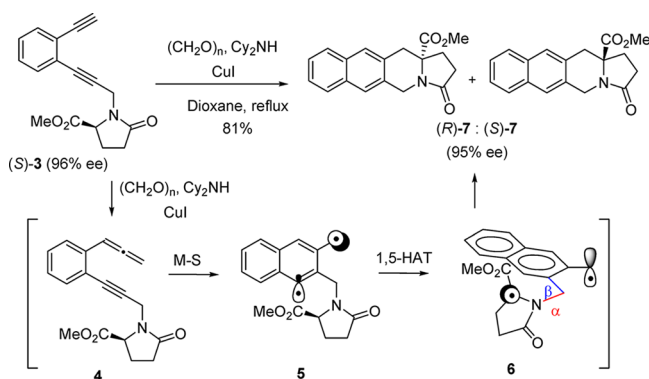


At this point, the choice of the proper terminology regarding the experimental results must be explained.<sup>9</sup> The concise and figurative expression of *memory of chirality* (MOC) was originally used to describe our experimental results.<sup>8</sup> This terminology introduced by Fuji and Kawabata is rather widespread in the literature.<sup>10</sup> This concept inspired our strategy. It was considered appropriate to our reaction, as during the process, (i) the static chirality of the starting material related to its chirogenic carbon center is destroyed, (ii) but the chirality is retained (memorized) via the generation of a transient radical intermediate where the new chirogenic element is an axis (dynamic chirality); (iii) the stereocenter is regenerated in the final product. It must be noted that the use of this idiomatic expression (MOC) has been severely criticized by Cozzi and

Received: June 30, 2014

Published: September 8, 2014

### Scheme 1. Rearrangement of Enediynes (S)-3: Proposed Mechanism



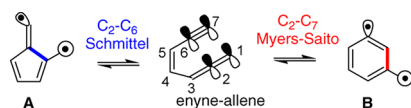
Siegel<sup>11</sup> and questioned by Wolf.<sup>12</sup> Since then, the term of MOC has been abandoned by Carlier<sup>10b,13</sup> who recommends the use of “self-regeneration of stereocenters via transient stereolabile intermediates”, which refers to the seminal work of Seebach.<sup>14</sup> The expression “memory of configuration” has also been adopted by Clayden.<sup>15</sup>

Back to our problem, to clearly demonstrate the mechanism of regeneration of the stereocenter, Crabbé's homologation of terminal alkynes was used for the in situ generation of achiral allene moieties from enantiopure enediynes such as compound 3.<sup>16</sup> As summarized in Scheme 1, the cascade rearrangement of 3 involves the formation of the nonisolable intermediate enyne-allene 4, which is followed successively by Myers–Saito cycloaromatization leading to the  $(\sigma,\pi)$  diradical 5, 1,5-hydrogen atom transfer, and eventually recombination of the resulting diradical 6. The model substrate 3 (96% ee) led to 7 in 81% yield with 95% ee (level of chirality transfer close to 99% within the limits of experimental errors). Due to stereoelectronic factors, intramolecular HAT from the stereogenic center to the  $\sigma$  radical center in 5 necessarily generates 6 in a native chiral conformation, and this dynamic chirality is preserved all along the recombination step. The nearly total level of preservation of chirality observed in this reaction was rationalized according to reasonable conjectures about the relative rates of rotation around  $\sigma$  bonds  $\alpha$  and  $\beta$  in the native conformation of diradical 6. This work reports a theoretical investigation of the three-step pathway leading from 4 to 7 in support to the origin of configurational memory in this rearrangement.<sup>17</sup>

### COMPUTATIONAL DETAILS

It is well established that, depending on their substitution pattern, enyne-allenes can undergo cycloaromatization, leading either to a six-membered  $(\sigma,\pi)$  1,4-diradical through  $C_2-C_7$  Myers–Saito<sup>3</sup> (M-S) reaction or to a five-membered  $(\sigma,\pi)$  1,4-diradical through  $C_2-C_6$  Schmittel<sup>18</sup> reaction (Scheme 2).<sup>19</sup>

### Scheme 2. Cyclization Pathways Transforming the Enyne-allene Framework into $(\sigma,\pi)$ 1,4-Diradicals A and B



The activation barrier is higher for Schmittel cyclization than for M-S rearrangement, which is the preferred pathway.<sup>20</sup> The singlet–triplet

(S-T) gap in both systems A and B is small because  $\sigma$  and  $\pi$  radical centers are orthogonal and through-bond spin-polarization is weak. Experimentally, the S-T gap in  $\alpha$ -3-didehydrotoluene B was estimated  $\leq 5$  kcal/mol.<sup>21</sup> MCSCF calculations indicated that the ground state is a singlet and that the S-T gap is  $-3.0$  kcal/mol.<sup>22</sup> In the M-S reaction, the reactant is a singlet closed-shell species, whereas the product is an open-shell singlet diradical. Moreover, the electronic population in the transition state is intermediate between a diradical state and a closed-shell state. Therefore, a multiconfigurational method is required for a correct description of transition states and diradical intermediates. High-level ab initio methods (CCSD(T), MR-MP2, ...) have been applied to model Schmittel and Myers–Saito reactions from the bare enyne-allene framework shown in Scheme 2.<sup>20,23</sup> Brueckner's approach<sup>24</sup> derived from the coupled-cluster<sup>25</sup> method has led to very good quantitative results on this model compound. It must be pointed out that geometry optimizations with these methods are too time-consuming to be applied to compounds 3–7. However, at the same time, the singlet diradicals have a typical two-configurational character that can only correctly be taken into account by a multideterminantal method. In other words, it was necessary to find a compromise. Whereas a monodeterminantal description of substituted enyne-allene derivatives with DFT methods is not a priori the best methodological choice, some recent works using the unrestricted broken spin-symmetry DFT (UBS-DFT) method on large substituted enediynes (Bergman cyclization) and enyne-allenes (Myers–Saito and Schmittel rearrangements) have led to valuable qualitative results.<sup>26–28</sup> For this reason, to investigate the rearrangement of enyne-allene 4, stationary points were located on the potential energy surface (PES) by using the restricted M06-2X/6-31G(d) method<sup>29</sup> for closed-shell species and the UBS-M06-2X/6-31G(d) method for diradical species and transition states. Calculations were performed with the Gaussian09 program package.<sup>30</sup> As the reaction occurs in apolar solvents (benzene or dioxane), calculations were carried out in vacuum. All stationary points (transition states and minima) were confirmed by a frequency calculation. The intrinsic reaction coordinate (IRC) was followed to validate transition states. The stability of the wave function was tested with STABLE=OPT keyword. As expected, spin contamination in the singlet ground state occurs. Pure diradical singlet states are not provided by

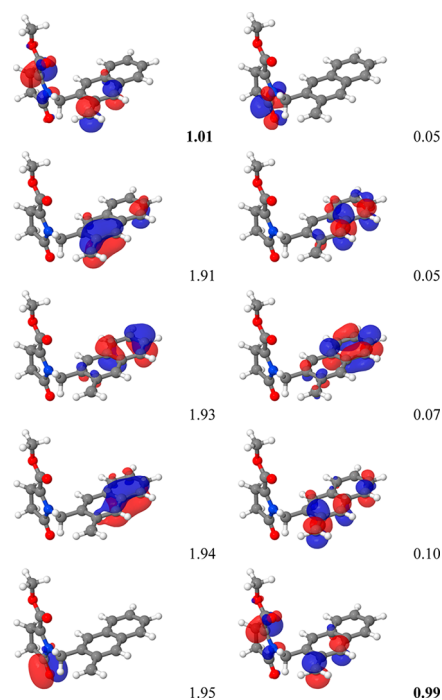
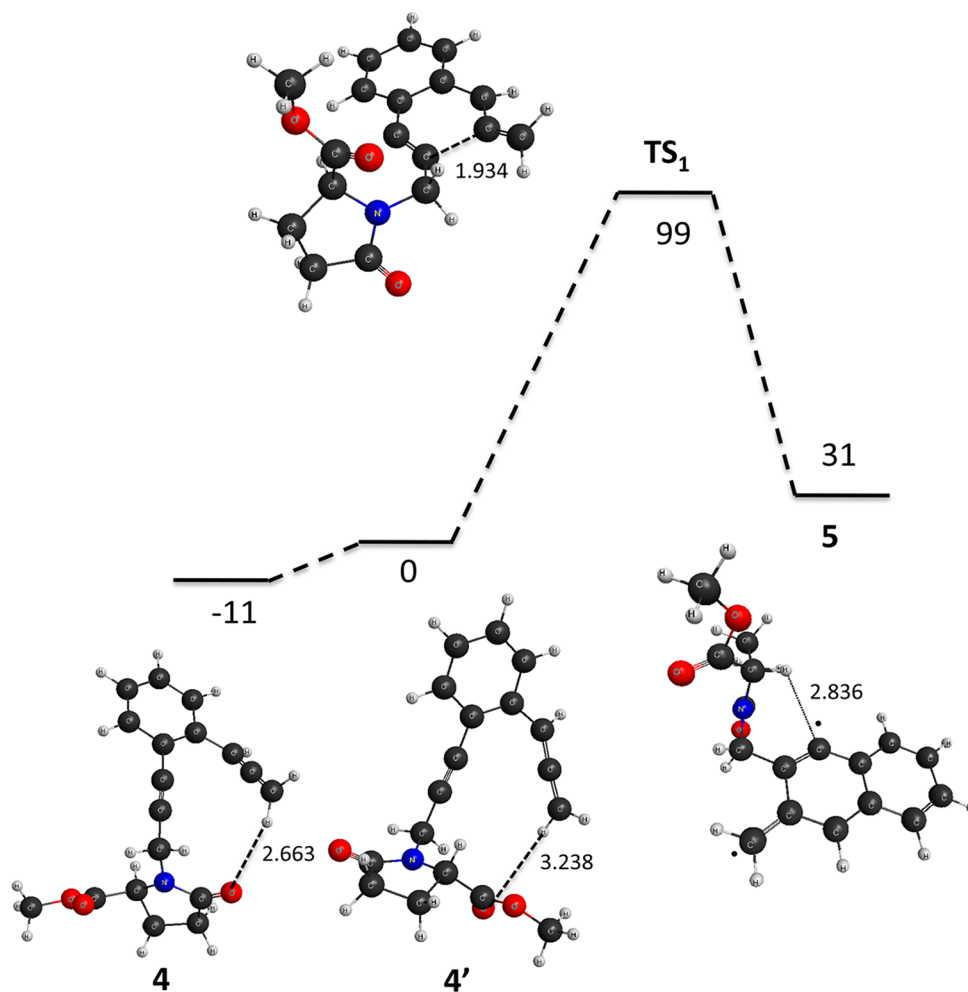


Figure 1. Selected natural orbitals of the active space and their occupancy in the case of diradical 6.



**Figure 2.** Reaction pathway leading to the  $(\sigma,\pi)$  diradical intermediate **5**. Relative  $\Delta G$  values are given in  $\text{kJ mol}^{-1}$  at room temperature and 1 atm at the MRPT2/6-31G(d)//CASSCF(10,10)/6-31G(d) level. Distances are given in Å.

this monodeterminantal method where  $\langle S^2 \rangle$  values are close to 1.0 for diradicals **5** and **6**.

To circumvent this problem, our choice was to carry out this study with a multireference method. Starting from these structures, all stationary points were reoptimized at the CASSCF(10,10)/6-31G(d) level.<sup>31</sup> Calculations were performed with GAMESS package.<sup>32</sup> Ten orbitals related to all valence  $\pi$  and  $\pi^*$  orbitals of enyne-allene **4** were included. As an illustration, these 10 orbitals correspond to the 10 orbitals shown in Figure 1 in the case of diradical **6**.

All configurations in the active space were generated. Only the singlet ground state was considered. All stationary points (transition states and minima) were confirmed by a frequency calculation. The intrinsic reaction coordinate (IRC) was again followed from the transition states to the reactants and the products. It is known that CASSCF activation energies are dramatically underestimated. Therefore, single point calculations at the multiconfigurational second-order perturbation theory MRPT2/6-31G(d)<sup>33</sup> level were performed to recover dynamic electron correlation. All given energies are  $\Delta G$  values at the MRPT2/6-31G(d)//CASSCF(10,10)/6-31G(d) level at 298.15 K and 1 atm.

## RESULTS AND DISCUSSION

As already stated, Myers–Saito (M-S) cycloaromatization is the very first step in the rearrangement of enantiopure enyne-allene intermediate (*S*)-**4** issued from Crabbé's homologation (Figures 2 and 3). The most stable conformation of enyne-allene (*S*)-**4** shows a stabilizing electrostatic interaction between the allenic proton and the carbonyl group of the cyclic amide ( $d(\text{H}\cdots\text{O}) = 2.663$  Å). The IRC calculation shows that the M-S

cycloaromatization proceeds via the less stable conformer (*S*)-**4'** which results from a  $180^\circ$  rotation around the  $\text{C}_{\text{sp}}-\text{CH}_2$  pivot. In both conformers (*S*)-**4** and (*S*)-**4'**, a dihedral angle of  $32^\circ$  is noted between the allenic moiety and the plane which contains the phenyl group conjugated to the triple bond. This value is larger than in hepta-1,2,4-trien-6-yne shown in Scheme 2 ( $\phi(\text{C}2-\text{C}3-\text{C}4-\text{C}5) = 24.7^\circ$  at the CASSCF(10,10)/6-31G(d) level<sup>20c</sup>) and can result from steric interactions between the allene framework and the substituted five-membered ring. Whereas the M-S reaction is exothermic by  $63 \text{ kJ mol}^{-1}$  for the above-mentioned parent system, the transformation of **4'** to **5** is slightly endothermic ( $19.5 \text{ kJ mol}^{-1}$ ). The cycloaromatization is the rate-determining step with a  $99 \text{ kJ mol}^{-1}$  activation free energy (Table 1, Figure 2) and a  $89 \text{ kJ mol}^{-1}$  ZPE-corrected activation energy. This value is consistent with the literature data reported for hepta-1,2,4-trien-6-yne. The activation free energy was determined experimentally ( $\Delta G_{298\text{K}}^\ddagger = 106 \pm 2 \text{ kJ mol}^{-1}$ ),<sup>34</sup> and the activation energy was calculated by Sakai and Nishitani at the MRPT2(10,10)/6-311+G(d,p) level ( $\Delta E_{0\text{K}}^\ddagger = 69 \text{ kJ mol}^{-1}$ ).<sup>20c,35</sup>

The transition state has a diradicaloid character (see the NOON and the calculated biradical character<sup>36</sup> in Table 1). In transition state  $\text{TS}_1$ , as in the reactant, the terminal allenic methylene is out of the plane formed by the conjugated moiety of the molecule with a dihedral angle of  $30^\circ$ . The methylene group has not fully rotated in the plane of the forming naphthyl

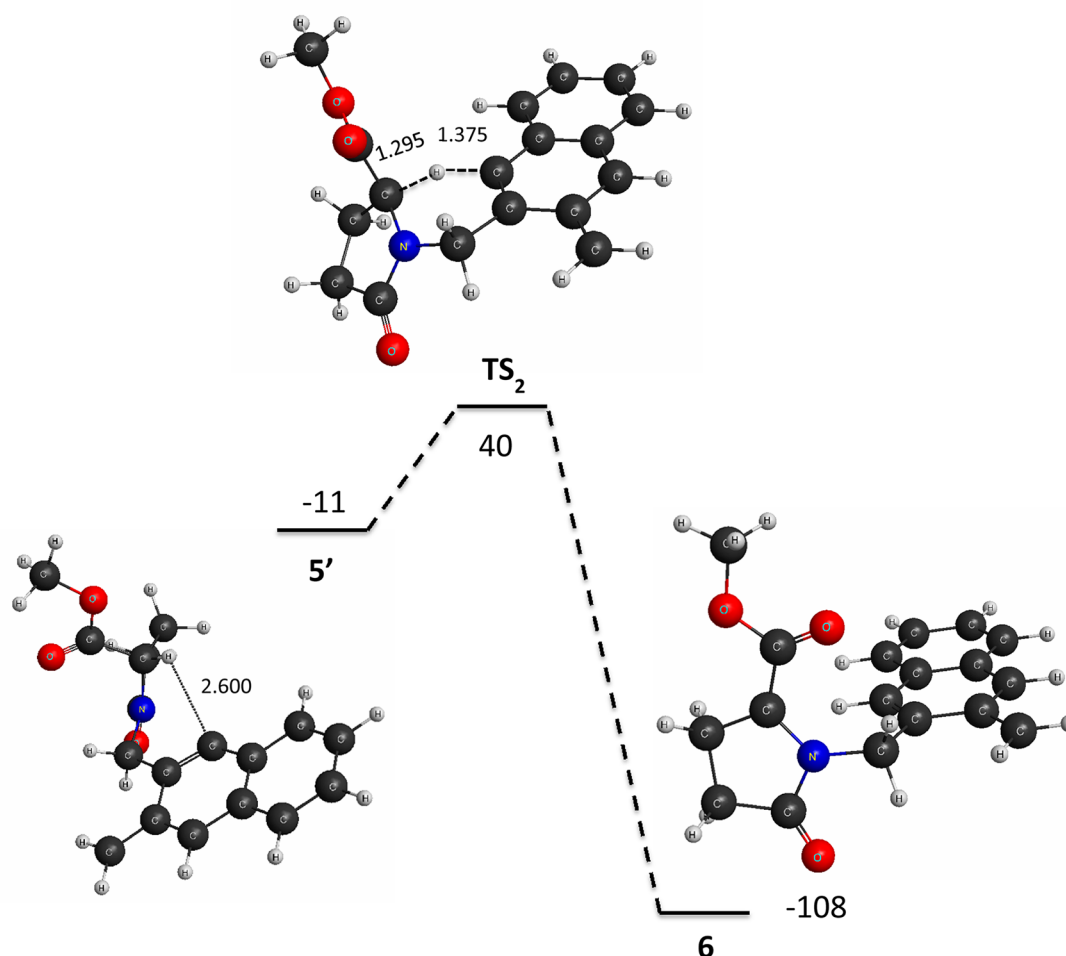


**Figure 3.** Intramolecular 1,5-HAT reaction pathway leading to the  $(\pi,\pi)$  diradical intermediate **6**. Relative  $\Delta G$  values are given in  $\text{kJ mol}^{-1}$  at room temperature and 1 atm at the MRPT2/6-31G(d)//CASSCF(10,10)/6-31G(d) level. Distances are given in Å.

ring. In  $\text{TS}_1$ , as in the resulting  $(\sigma,\pi)$  diradical **5**, the pyroglutamate ring adopts an envelope conformation where the  $\text{CH}_2$  group in the  $\beta$  position relative to the amide carbonyl group is out-of-plane. The methyl carboxylate group lies in an equatorial position. The pyroglutamate ring undergoes pseudorotation to adopt the envelope conformation **5'** (with the  $\text{CO}_2\text{Me}$  moiety in the axial position) more prone to evolve via 1,5-hydrogen atom transfer (HAT). This conformer is more stable by  $40 \text{ kJ mol}^{-1}$  than **5**, and the H atom in the captodative position is closer to the  $\sigma$  radical center (Figure 2). Intermediate **5'** is readily converted by intramolecular HAT ( $51 \text{ kJ mol}^{-1}$  activation free energy) into the highly stabilized  $(\pi,\pi)$  diradical **6** more stable by  $108 \text{ kJ mol}^{-1}$  than the reactive conformer **4'** of the enyne-allene (Figure 3).

The S-T gap in diradicals **5'** and **6** was calculated ( $-9$  and  $\sim 0 \text{ kJ mol}^{-1}$ , respectively). During the 1,5-HAT step, the static central chirality of diradical **5** is converted into the dynamic axial chirality of diradical **6**. In the native conformation of diradical **6** the naphthyl group and the five-membered ring are orthogonal. Both singly occupied orbitals are degenerate. They have a  $\pi$  character and are delocalized for both radical centers which are planar (Figure 4). The largest coefficients correspond to the p orbitals located on the carbon and the nitrogen atoms in regard to the captodative moiety; the benzylic radical center is stabilized by conjugation with the naphthyl group (the main contribution comes from the ortho aromatic C(H)).

At this stage of the process, rotations around sigma bonds  $\alpha$  and  $\beta$  (Scheme 1) can both formally occur on the route to the final product **7** by intramolecular coupling of the two radical centers (Scheme 3, Figure 4b,c). Whereas a rotation around the bond  $\beta$  can itself lead to (*R*)-**7**, the rotation around bond  $\alpha$  cannot; the latter must necessarily be accompanied by a rotation around bond  $\beta$ .

Rotation around the C–N bond  $\alpha$  either clockwise or counterclockwise is sterically impeded (huge steric interaction between the naphthyl moiety and the substituents of the rotating five-membered ring). A relaxed manual rotation with a step of  $1^\circ$  was performed in the triplet configuration at UM06-2X/6-31G(d) level because of convergence problems in the diradical singlet state. The results clearly showed that the two moieties bump into each other, and even the less energy demanding counterclockwise rotation around the C–N bond cannot proceed without concomitant rotation around the C–C bond  $\beta$ . As soon as the  $\varphi(\text{C}-\text{CH}_2-\text{N}-\text{C}(=\text{O}))$  dihedral angle is reduced from  $98^\circ$  to  $53^\circ$ , the distance between the intracyclic carbonyl group and the naphthyl ring is close to  $3 \text{ \AA}$  and a rotation around the C–C bond is required to reduce steric hindrance.<sup>37</sup> Therefore, such a pathway, which would finally induce the formation of (*S*)-**7**, cannot contribute to the formation of **7**.

Conversely two competitive rotations around the C–C bond  $\beta$  can be considered: clockwise rotation (Scheme 3, Table 1, Figure 5,  $\text{TS3b} \rightarrow \mathbf{6b}$ ) and counterclockwise rotation (Scheme 3,



Table 1. Thermodynamic and Electronic Data Relative to Compounds 4 to 7

compound	relative $\Delta G$ values <sup>a</sup> (kJ mol <sup>-1</sup> )	S-T gap <sup>b</sup> (kJ mol <sup>-1</sup> )	NOON <sup>c</sup>	biradical character $\gamma^d$ (%)
4	-11	–	1.92; 0.09	0
4'	0	–	1.92; 0.08	0
TS <sub>1</sub>	99	–	1.75; 0.25	4
5	31	–	1.03; 0.97	94
5'	-11	-9	1.02; 0.98	96
TS <sub>2</sub>	40	–	1.03; 0.97	94
6	-108	~0	1.01; 0.99	98
TS <sub>3a</sub>	39	–	1.03; 0.97	94
6a	-7	-102	1.02; 0.98	96
7'	-363	–	1.89; 0.12	1
TS <sub>3b</sub>	<0.5	–	1.02; 0.98	96
6b	-14	-12	1.15; 0.85	71
7	-304	–	1.92; 0.08	0

<sup>a</sup>Relative  $\Delta G$  values at room temperature at the MRPT2/6-31G(d)//CASSCF(10,10)/6-31G(d) level. <sup>b</sup>A negative value for the S-T gap corresponds to a more stable singlet state. <sup>c</sup>Natural orbital occupation number (NOON) for frontier orbitals, i.e., the pair of natural orbitals with an occupation number close to one for diradicals and diradicaloid structures and HOMO–LUMO orbitals for closed-shell species. <sup>d</sup>The  $\gamma$  value is given by the following formula:  $\gamma = 1 - 4|\Delta_{\text{NOON}}|/(4 + \Delta_{\text{NOON}}^2)$ .<sup>35</sup>

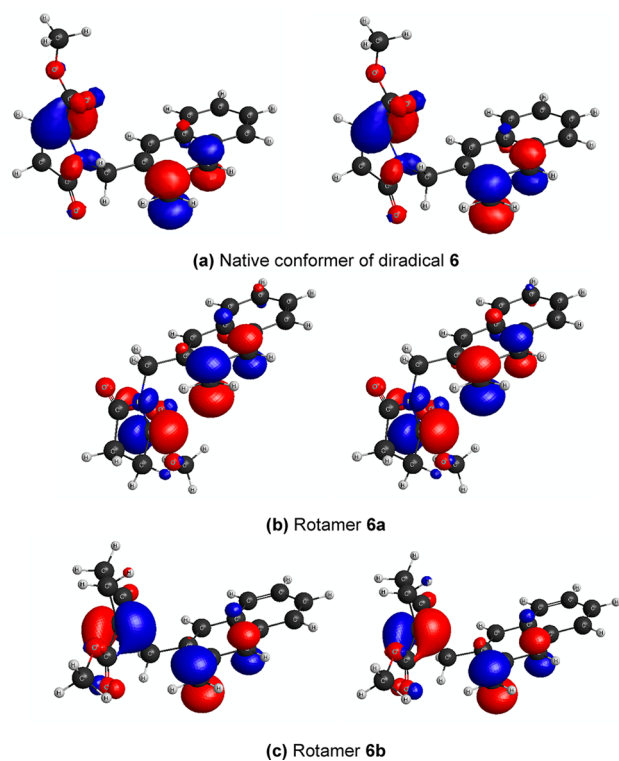


Figure 4. Pairs of natural orbitals with an occupation number close to one. (a) Native conformer of ( $\pi,\pi$ ) diradical 6. (b) Rotamer 6a. (c) Rotamer 6b.

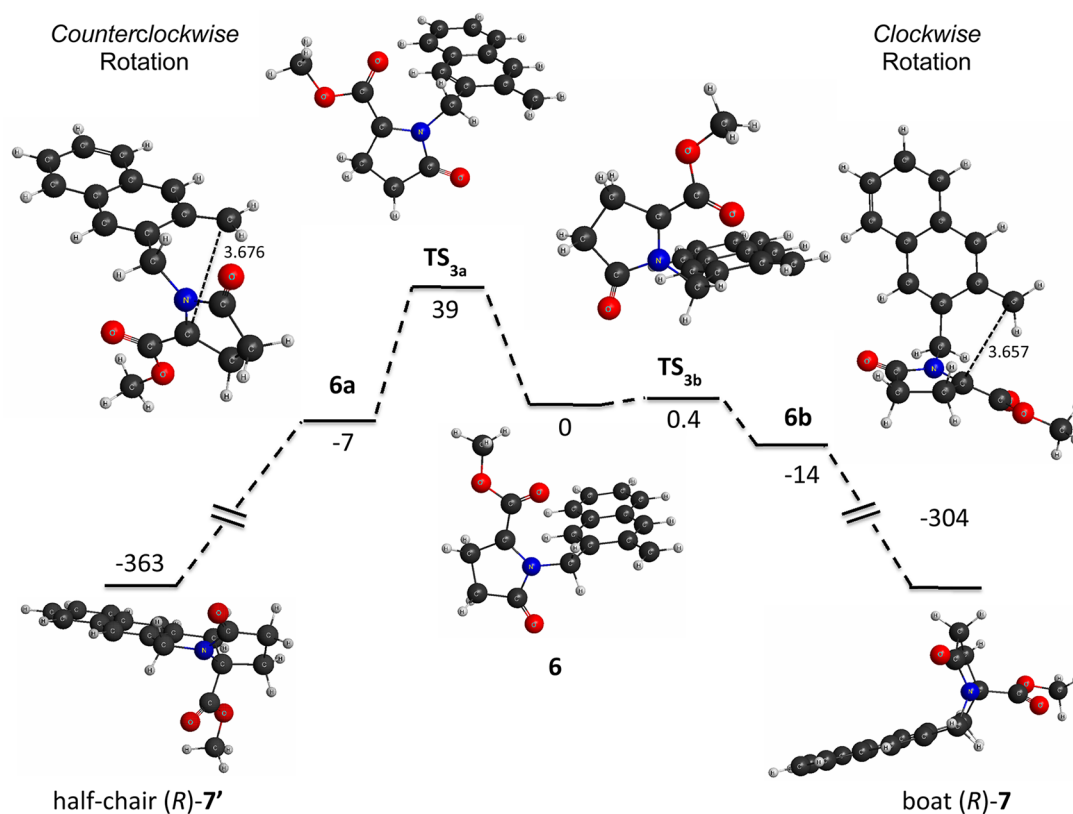
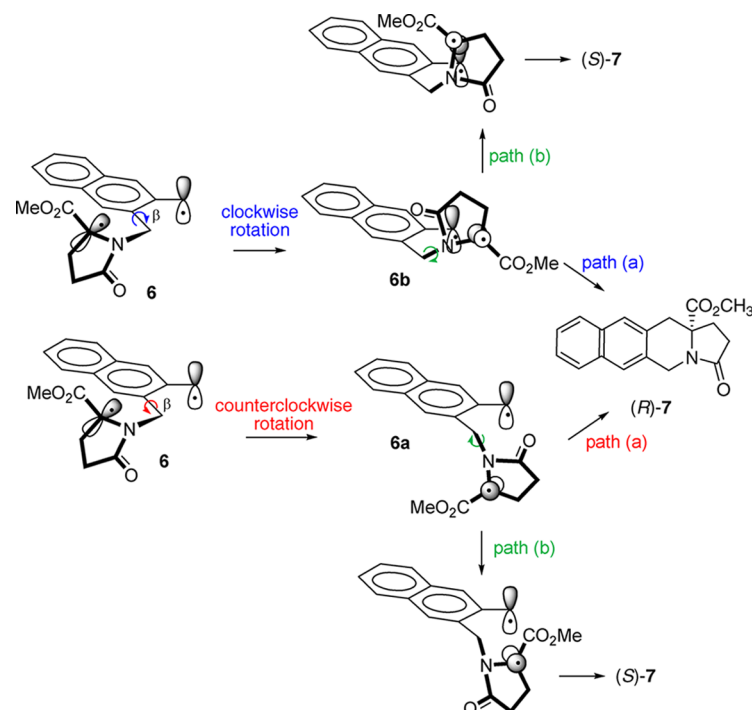
Table 1, Figure 5, TS<sub>3a</sub> → 6a). To locate the corresponding transition structures, a first computation on the triplet wave function followed by swapping to the proper open-shell singlet state was preferred. The clockwise rotation (TS<sub>3b</sub>) has a negligible free activation energy (0.4 kJ mol<sup>-1</sup>) and leads through transition state TS<sub>3b</sub> to intermediate 6b. Comparatively, the counterclockwise rotation has a 39 kJ mol<sup>-1</sup> activation barrier (the structure of TS<sub>3a</sub> reveals some steric hindrance between the CO<sub>2</sub>Me group and the naphthyl moiety). It leads to intermediate 6a which is slightly more energetic than 6b. So the latter is both kinetically and thermodynamically favored. Some

discrepancies can be pointed out in the geometry as well as in the electronic structure of intermediates 6a and 6b (Table 1, Figure 6).

According to the NOON values, intermediate 6a has a more pronounced diradical character. Moreover, if one considers only HOMO/LUMO orbitals referred to as 1/2, the CAS wave function can be written as 0.207|11̄̄| - 0.193|22̄̄| - 0.601|2̄1̄| + 0.601|12̄̄|. The two first terms can be considered as polarization terms, and they have a low contribution. On the contrary, intermediate 6b is more polarized and the polarization terms have the largest CAS coefficients: 0.616|11̄̄| - 0.509|22̄̄| - 0.290|2̄1̄| - 0.290|12̄̄|. The electronic structure of 6b is therefore closer to that of the final product (*R*)-7. Concerning the geometry, dihedral angles around pivots  $\alpha$  and  $\beta$  (noted  $\varphi(\text{C}-\text{CH}_2-\text{N}-\text{C}(\text{=O}))$  and  $\varphi(\text{C}(\text{H})-\text{C}-\text{CH}_2-\text{N})$ , respectively) are very different in 6a and 6b:  $\varphi(\text{C}-\text{CH}_2-\text{N}-\text{C}(\text{=O})) = 126^\circ$  and  $\varphi(\text{C}(\text{H})-\text{C}-\text{CH}_2-\text{N}) = 135^\circ$  in 6a. The dihedral angles determined for 6b ( $\varphi(\text{C}-\text{CH}_2-\text{N}-\text{C}(\text{=O})) = 80^\circ$  and  $\varphi(\text{C}(\text{H})-\text{C}-\text{CH}_2-\text{N}) = -90^\circ$ ) lead to the conclusion that in this case the two rings are really orthogonal, and this is in agreement with its low S-T gap.

It is of prime importance to notice that whatever the direction of the rotation the same (*R*)-enantiomer of the final product is formed although in a different conformation (7 or 7') (Figure 5). Inversion of configuration cannot be expected. At best, partial racemization might result from initial rotation around bond  $\beta$  leading to 6b (and or 6a) followed by rotation around bond  $\alpha$ . As shown in Scheme 3, as the rotation around the C–C pivot proceeds, a rotation around the C–N bond requiring less energy might be envisaged.

The very last part of the intramolecular coupling occurs without any activation energy from both localized stationary points 6a and 6b (Scheme 3, Figure 5). No transition state on the PES could be located at the MRPT2/6-31G(d)//CASSCF(10,10)/6-31G(d) level of calculation. As already stated, the two directions of rotation lead to the (*R*)-isomer of the final product 7. This justifies why chirality is fully maintained throughout the whole process. The clockwise rotation via 6b leads to the fused-piperidine ring of the final product (*R*)-7 in a boat conformation that can easily convert to the thermodynamic conformer (*R*)-7' whereas the counterclockwise rotation via 6a leads directly to the more stable half-chair conformation of the final product.

Scheme 3. Investigated Rotations around the Two  $\sigma$  Bond Pivots in the Intermediate  $(\pi,\pi)$  Diradical  $6^a$ 

**Figure 5.** Clockwise and counterclockwise rotations around the C-C bond  $\beta$  in  $(\pi,\pi)$  diradical  $6$ , leading to the final product  $(R)$ -7. Relative  $\Delta G$  values in  $\text{kJ mol}^{-1}$  at room temperature and 1 atm at the MRPT2/6-31G(d)//CASSCF(10,10)/6-31G(d) level. Distances are given in  $\text{\AA}$ .

Any partially racemizing route leading to the  $(S)$ -enantiomer of the final product  $7$  (path b) would necessarily imply an additional rotation around the C-N pivot, i.e., an additional energetic cost compared to path a. Due to the very low activation

barrier calculated for the clockwise rotation in path a, the formation of  $(S)$ -7 is highly unlikely.<sup>38</sup> The observed rearrangement obeys the “least motion principle”,<sup>39</sup> and the level of chirality transfer reaches 99%.

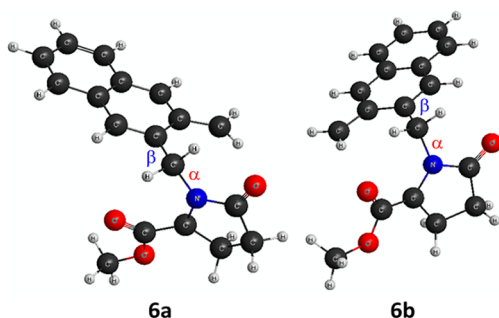


Figure 6. Structures of ( $\pi,\pi$ ) diradical conformers **6a** and **6b** at the CASSCF(10,10)/6-31G(d) level of calculation.

## CONCLUSION

The entire description of the three-step transformation leading from enyne-allene **4** to (*R*)-**7** was achieved by using MRPT2/6-31G(d)//CASSCF(10,10)/6-31G(d) calculations selected to correctly account for the optimized geometries and energetics of the pure ground-state singlet species (diradicals, diradicaloid transition state, diradical transition states, and closed-shell systems) involved in the reaction path. The extremely low rotational barrier around the benzylic C–C pivot (bond  $\beta$ ), which excludes rotation around the second  $\sigma$  pivot (C–N bond  $\alpha$ ) in the conformationally chiral diradical intermediate **6**, explains how the chirality is stored and evolves throughout the multistep radical rearrangement, in other words it provides a rationale to the configurational memory observed in this process. Both clockwise and counterclockwise rotations around the C–C bond account for the formation of the enantiopure (*R*)-product in the critical recombination step. However, the experimentally observed retention of configuration is more likely to result from the clockwise rotation mode, as the free energy of the corresponding transition state ( $\text{TS}_{3a}$ ) was found significantly lower than that of the counterclockwise rotation mode ( $\text{TS}_{3b}$ ).

## ASSOCIATED CONTENT

### Supporting Information

Structures, MRPT2 energies, and Gibbs free energy correction values for all stationary points at the MRPT2/6-31G(d)//CASSCF(10,10)/6-31G(d) level of calculation; structures and energy values for transition states located in triplet configuration at the UM06-2X/6-31G(d) level of calculation. This material is available free of charge via the Internet at <http://pubs.acs.org>.

## AUTHOR INFORMATION

### Corresponding Author

\*E-mail: [anouk.siri@univ-amu.fr](mailto:anouk.siri@univ-amu.fr).

### Notes

The authors declare no competing financial interests.

## ACKNOWLEDGMENTS

The authors acknowledge Professor C. Roussel for stimulating comments. This work was supported by the computing facilities of the CRCMM, “Centre Régional de Compétences en Modélisation Moléculaire de Marseille”. The authors thank Aix-Marseille University, CNRS, for financial support. DST (Government of India) is also acknowledged for financial support to S.M. through Inspire Faculty Award.

## REFERENCES

- (1) (a) Smith, A. L.; Nicolaou, K. C. *J. Med. Chem.* **1996**, *39*, 2103–2117 and references therein. (b) Nicolaou, K. C.; Dai, W. M. *Angew. Chem., Int. Ed. Engl.* **1991**, *30*, 1387–1416 and references therein. (c) Nicolaou, K. C.; Dai, W. M.; Tsay, S. C.; Estevez, V. A.; Wrasidlo, W. *Science* **1992**, *256*, 1172–1178. (d) Ahlert, J.; Shepard, E.; Lomovskaya, N.; Zazopoulos, E.; Staffa, A.; Bachmann, B. O.; Huang, K.; Fonstein, L.; Czisny, A.; Whitwam, R. E.; Farnet, C. M.; Thorson, J. S. *Science* **2002**, *297*, 1173–1176.
- (2) Jones, R.; Bergman, R. G. *J. Am. Chem. Soc.* **1972**, *94*, 660–661.
- (3) (a) Myers, A. G.; Kuo, E. Y.; Finney, N. S. *J. Am. Chem. Soc.* **1989**, *111*, 8057–8059. (b) Myers, A. G.; Dragovich, P. S.; Kuo, E. Y. *J. Am. Chem. Soc.* **1992**, *114*, 9369–9386. (c) Nagata, R.; Yamanaka, H.; Murahashi, E.; Saito, I. *Tetrahedron Lett.* **1990**, *31*, 2907–2910.
- (4) (a) Hamann, P. R.; Upešlacis, J.; Borders, D. B. In *Anticancer Agents from Natural Products*, 2nd ed.; Cragg, G. M.; Kingston, D. G. I.; Newman, D. J., Eds.; CRC Press: Boca Raton, FL, 2012; pp 575–621. (b) Breiner, B.; Kaya, K.; Roy, S.; Yang, W.-Y.; Alabugin, I. V. *Org. Biomol. Chem.* **2012**, *10*, 3974–3987. (c) Joshi, M. C.; Rawat, D. S. *Chem. Biodiversity* **2012**, *9*, 459–498. (d) Polukhtina, A.; Karpov, G.; Pandithavidana, D. R.; Kuzmin, A.; Popik, V. V. *Aust. J. Chem.* **2010**, *63*, 1099–1107. (e) Toshima, K. *Synlett* **2012**, *23*, 2025–2052. (f) Shao, R.-G. *Curr. Mol. Pharmacol.* **2008**, *1*, 50–60. (g) Kar, M.; Basak, A. *Chem. Rev.* **2007**, *107*, 2861–2890.
- (5) (a) Xiao, Y.; Hu, A. *Macromol. Rapid Commun.* **2011**, *32*, 1688–1698. (b) Boerner, L. J. K.; Dye, D. F.; Kopke, T.; Zaleski, J. M. *Coord. Chem. Rev.* **2013**, *257*, 599–620. (c) Li, Z.; Song, D.; Zhi, J.; Hu, A. *J. Phys. Chem. C* **2011**, *115*, 15829–15833. (d) Sun, S.; Zhu, C.; Song, D.; Li, F.; Hu, A. *Polym. Chem.* **2014**, *5*, 1241–1247. (e) Yang, X.; Li, Z.; Zhi, J.; Ma, J.; Hu, A. *Langmuir* **2010**, *26*, 11244–11248. (f) Ito, S.; Iida, T.; Kawakami, J.; Okujima, T.; Morita, N. *Eur. J. Org. Chem.* **2009**, *31*, 5355–5364. (g) Mondal, S.; Dumur, F.; Barbarat, B.; Grauby, O.; Gignes, D.; Olive, D.; Bertrand, M. P.; Nechab, M. *Colloids Surf., B* **2013**, *112*, 513–520.
- (6) (a) Kraka, E.; Cremer, D. *WIREs Comput. Mol. Sci.* **2013**, DOI: 10.1002/wcms.1174. (b) Schreiner, P. R.; Navarro-Vazquez, A.; Prall, M. *Acc. Chem. Res.* **2005**, *38*, 29–37. (c) Gräfenstein, J.; Kraka, E.; Filatov, M.; Cremer, D. *Int. J. Mol. Sci.* **2002**, *3*, 360–394.
- (7) For a recent review on chirality transfer, see: Campolo, D.; Gastaldi, S.; Roussel, C.; Bertrand, M. P.; Nechab, M. *Chem. Soc. Rev.* **2013**, *42*, 8434–8466.
- (8) (a) Nechab, M.; Campolo, D.; Maury, J.; Perfetti, P.; Vanthuyne, N.; Siri, D.; Bertrand, M. P. *J. Am. Chem. Soc.* **2010**, *132*, 14742–14744. (b) Nechab, M.; Besson, E.; Campolo, D.; Perfetti, P.; Vanthuyne, N.; Bloch, E.; Denoyel, R.; Bertrand, M. P. *Chem. Commun.* **2011**, *47*, 5286–5288. (c) Campolo, D.; Gaudel-Siri, A.; Mondal, S.; Siri, D.; Besson, D.; Vanthuyne, N.; Nechab, M.; Bertrand, M. P. *J. Org. Chem.* **2012**, *77*, 2773–2783. (d) Mondal, S.; Nechab, N.; Campolo, D.; Vanthuyne, N.; Bertrand, M. P. *Adv. Synth. Catal.* **2012**, *354*, 1987–2000.
- (9) This digression was included to address a reviewer’s remark and draw the reader’s attention to the importance for the scientific writer to use appropriate terms and evaluate the risk of propagating metaphors that might be misinterpreted.
- (10) (a) Fujii, K.; Kawabata, T. *Chem.—Eur. J.* **1998**, *4*, 373–376. (b) Zhao, H.; Hsu, D. C.; Carlier, P. R. *Synthesis* **2005**, *1*, 1–16. (c) Kawabata, T.; Fujii, K. In *Topics in Stereochemistry*; Denmark, S. E., Ed.; Wiley and Sons Inc.: New York, 2003, Vol. 23, pp 175–205.
- (11) Cozzi, F.; Siegel, J. S. *Org. Biomol. Chem.* **2005**, *3*, 4296–4298.
- (12) Wolf, C. In *Dynamic Stereochemistry of Chiral Compounds: Principles and Applications*; Royal Society of Chemistry: Cambridge, UK, 2008; pp 282–289.
- (13) (a) Carlier, P. R.; Hsu, D. C.; Bryson, S. A. In *Stereochemical Aspects of Organolithium Compounds*; Gawley, R. E., Ed.; Topics in Stereochemistry; Siegel, J. S., Series, Ed.; Verlag Helvetica Chimica Acta: Zürich, 2010; Vol. 26, pp 53–92. (b) Carlier, P. R.; Sun, Y.-S.; Hsu, D. C.; Chen, Q.-H. *J. Org. Chem.* **2010**, *75*, 6588–6594.
- (14) Seebach, D.; Wasmuth, D. *Angew. Chem., Int. Ed.* **1981**, *20*, 971.



- (15) Fletcher, S. P.; Solà, J.; Holt, D.; Brown, R. A.; Clayden, J. *Belstein J. Org. Chem.* **2011**, *7*, 1304–1309.
- (16) Mondal, S.; Nechab, M.; Vanthuyne, N.; Bertrand, M. P. *Chem. Commun.* **2012**, *48*, 2549–2551.
- (17) For a theoretical support to the origin of memory of chirality in Norrish–Yang cyclization, see: (a) Giese, B.; Wettstein, P.; Stähelin, C.; Barbosa, F.; Neuburger, M.; Zehnder, M.; Wessig, P. *Angew. Chem., Int. Ed.* **1999**, *38*, 2586–2587. (b) Sinicropi, A.; Barbosa, F.; Basosi, R.; Giese, B.; Olivucci, M. *Angew. Chem., Int. Ed.* **2005**, *44*, 2390–2393.
- (18) (a) Schmittel, M.; Strittmatter, M.; Kiau, S. *Tetrahedron Lett.* **1995**, *36*, 4975–4978. (b) Schmittel, M.; Kiau, S.; Siebert, T.; Strittmatter, M. *Tetrahedron Lett.* **1996**, *37*, 7691–7694. (c) Schreiner, P. R.; Prall, M. *J. Am. Chem. Soc.* **1999**, *121*, 8615–8627.
- (19) For general reviews, see: (a) Mohamed, R. K.; Peterson, P. W.; Alabugin, I. V. *Chem. Rev.* **2013**, *113*, 7089–7129. (b) Peterson, P. W.; Mohamed, R. K.; Alabugin, I. V. *Eur. J. Org. Chem.* **2013**, *13*, 2505–2527. (c) Navarro-Vazquez, A.; Prall, M.; Schreiner, P. R. *Org. Lett.* **2004**, *6*, 2981–2984. (d) Alabugin, I. V.; Breiner, B.; Manoharan, M. *Adv. Phys. Org. Chem.* **2008**, *42*, 1–33.
- (20) (a) De Visser, S. P.; Filatov, M.; Shaik, S. *Phys. Chem. Chem. Phys.* **2001**, *3*, 1242–1245. (b) Prall, M.; Wittkopp, A.; Schreiner, P. R. *J. Phys. Chem. A* **2001**, *105*, 9265–9274. (c) Sakai, S.; Nishitani, M. *J. Phys. Chem. A* **2010**, *114*, 11807–11813.
- (21) Logan, C. F.; Ma, J. C.; Chen, P. J. *Am. Chem. Soc.* **1994**, *116*, 2137–2138.
- (22) (a) Wenthold, P. G.; Wierschke, S. G.; Nash, J. J.; Squires, R. J. *Am. Chem. Soc.* **1993**, *115*, 12611–12612. (b) Wenthold, P. G.; Wierschke, S. G.; Nash, J. J.; Squires, R. J. *Am. Chem. Soc.* **1994**, *116*, 7378–7392.
- (23) For a recent application to Bergman cyclization, see: Greer, E. M.; Cosgriff, C. V.; Doubleday, C. *J. Am. Chem. Soc.* **2013**, *135*, 10194–10197.
- (24) (a) Kobayashi, R.; Handy, N. C.; Amos, R. D.; Trucks, G. W.; Frisch, M. J.; Pople, J. A. *J. Chem. Phys.* **1991**, *95*, 6723–6733. (b) Crawford, T. D.; Lee, T. J.; Handy, N. C.; Schaefer, H. F., III. *J. Chem. Phys.* **1997**, *107*, 9980–9984. (c) Lindgren, I.; Salomonson, S. *Int. J. Quantum Chem.* **2002**, *90*, 294–316.
- (25) (a) Purvis, G. D., III; Bartlett, R. J. *J. Chem. Phys.* **1982**, *76*, 1910–1918. (b) Čížek, J. In *Advances in Chemical Physics: Correlation Effects in Atoms and Molecules*; LeFebvre, R.; Moser, C., Eds.; John Wiley & Sons, Inc.: Hoboken, NJ, 2007; Vol. 14, pp 35–89.
- (26) (a) Ess, D. H.; Johnson, E. R.; Hu, X.; Yang, W. *J. Phys. Chem. A* **2011**, *115*, 76–83. (b) Lim, M. H.; Worthington, S. E.; Dulles, F. J.; Cramer, C. J. In *Chemical Applications of Density-Functional Theory*; Laird, B. B.; Ross, R. B.; Ziegler, T., Eds.; American Chemical Society: Washington, DC, 1996; Chapter 27, pp 402–422.
- (27) (a) Baroudi, A.; Mauldin, J.; Alabugin, I. V. *J. Am. Chem. Soc.* **2010**, *132*, 967–979. (b) Zeidan, T. A.; Manoharan, M.; Alabugin, I. V. *J. Org. Chem.* **2006**, *71*, 954–961. (c) Zeidan, T. A.; Kovalenko, S. V.; Manoharan, M.; Alabugin, I. V. *J. Org. Chem.* **2006**, *71*, 962–975. (d) Alabugin, I. V.; Manoharan, M.; Kovalenko, S. V. *Org. Lett.* **2002**, *4*, 1119–1122. (e) Kraka, E.; Cremer, D. *J. Am. Chem. Soc.* **2000**, *122*, 8245–8264. (f) Gräfenstein, J.; Hjerpe, A. M.; Kraka, E.; Cremer, D. *J. Phys. Chem. A* **2000**, *104*, 1748–1761.
- (28) (a) Basak, A.; Das, S.; Mallick, D.; Jemmis, E. D. *J. Am. Chem. Soc.* **2009**, *131*, 15695–15704. (b) Bekele, T.; Christian, C. F.; Lipton, M. A.; Singleton, D. A. *J. Am. Chem. Soc.* **2005**, *127*, 9216–9223. (c) Alabugin, I. V.; Manoharan, M. *J. Am. Chem. Soc.* **2003**, *125*, 4495–4509. (d) Chen, W.-C.; Zou, J.-W.; Yu, C.-H. *J. Org. Chem.* **2003**, *68*, 3663–3672.
- (29) Zhao, Y.; Truhlar, D. *Acc. Chem. Res.* **2008**, *41*, 157–167.
- (30) Frisch, M. J.; Trucks, G. W.; Schlegel, H. B.; Scuseria, G. E.; Robb, M. A.; Cheeseman, J. R.; Scalmani, G.; Barone, V.; Mennucci, B.; Petersson, G. A.; Nakatsuji, H.; Caricato, M.; Li, X.; Hratchian, H. P.; Izmaylov, A. F.; Bloino, J.; Zheng, G.; Sonnenberg, J. L.; Hada, M.; Ehara, M.; Toyota, K.; Fukuda, R.; Hasegawa, J.; Ishida, M.; Nakajima, T.; Honda, Y.; Kitao, O.; Nakai, H.; Vreven, T.; Montgomery, J. A., Jr.; Peralta, J. E.; Ogliaro, F.; Bearpark, M.; Heyd, J. J.; Brothers, E.; Kudin, K. N.; Staroverov, V. N.; Kobayashi, R.; Normand, J.; Raghavachari, K.; Rendell, A.; Burant, J. C.; Iyengar, S. S.; Tomasi, J.; Cossi, M.; Rega, N.; Millam, N. J.; Klene, M.; Knox, J. E.; Cross, J. B.; Bakken, V.; Adamo, C.; Jaramillo, J.; Gomperts, R.; Stratmann, R. E.; Yazyev, O.; Austin, A. J.; Cammi, R.; Pomelli, C.; Ochterski, J. W.; Martin, R. L.; Morokuma, K.; Zakrzewski, V. G.; Voth, G. A.; Salvador, P.; Dannenberg, J. J.; Dapprich, S.; Daniels, A. D.; Farkas, Ö.; Foresman, J. B.; Ortiz, J. V.; Cioslowski, J.; Fox, D. J. *Gaussian 09, Revision D.01*, Gaussian, Inc., Wallingford, CT, 2009.
- (31) (a) Roos, B. O. In *Advances in Chemical Physics: Ab Initio Methods in Quantum Chemistry Part 2*; Lawley, K. P., Eds.; John Wiley & Sons, Inc.: Hoboken, NJ, 2007; Vol. 69, pp 399–445. (b) Yamamoto, N.; Vreven, T.; Robb, M. A.; Frisch, M. J.; Schlegel, H. B. *Chem. Phys. Lett.* **1996**, *250*, 373–378.
- (32) Schmidt, M. W.; Baldrige, K. K.; Boatz, J. A.; Elbert, S. T.; Gordon, M. S.; Jensen, J. H.; Kosecki, S.; Matsunaga, N.; Nguyen, K. A.; Su, S. J.; Windus, T. L.; Dupuis, M.; Montgomery, J. A. *J. Comput. Chem.* **1993**, *14*, 1347–1363.
- (33) Nakano, H. *J. Chem. Phys.* **1993**, *99*, 7983–7992.
- (34) Myers, A. G.; Dragovich, P. S.; Kuo, E. Y. *J. Am. Chem. Soc.* **1992**, *114*, 9369–9386.
- (35) For a more detailed comparison of computed values using various methodologies, see refs 6a, 6b, 14a, 14c, and references cited therein.
- (36) Kamada, K.; Ohta, K.; Shimizu, A.; Kubo, T.; Kishi, R.; Takahashi, H.; Botek, E.; Champagne, B.; Nakano, M. *J. Phys. Chem. Lett.* **2010**, *1*, 937–940.
- (37) The four transition states corresponding to the clockwise and counterclockwise rotations around bonds  $\alpha$  and  $\beta$  were located at the UM06-2X/6-31G(d) level of calculation in their triplet configuration. Single point energy calculations at the UBS-M06-2X/6-31G(d) level of calculation provided the energy of the spin-contaminated singlet transition states ( $\langle S^2 \rangle$  value close to 1). Both are highly energetic for clockwise/counterclockwise rotations around bond  $\alpha$  (40.0/23.5 kJ·mol<sup>-1</sup> above ( $\pi,\pi$ ) diradical intermediate **6**, respectively), as compared to those corresponding to clockwise/counterclockwise rotations around bond  $\beta$  (2.5/6.6 kJ·mol<sup>-1</sup> above intermediate **6** at this level of calculation, respectively).
- (38) The rotation around bond  $\alpha$  was investigated starting from structure **6b**. Both transition states in triplet configuration for the clockwise and counterclockwise rotations around the C–N bond  $\alpha$  were located at the UM06-2X/6-31G(d) level of calculation. Single point energy calculations at the UBS-M06-2X/6-31G(d) level of calculation provided the energy of the spin-contaminated singlet transition states ( $\langle S^2 \rangle$  value close to 1). Free energy values are 33.7/44.7 kJ·mol<sup>-1</sup> above ( $\pi,\pi$ ) diradical intermediate **6b** for clockwise/counterclockwise rotations respectively. It must be noted that this methodology allowed the location of a transition state for the coupling leading to (R)-7. The free energy value of this stationary point was found only 23.2 kJ·mol<sup>-1</sup> above **6b** at this level of calculation.
- (39) According to Hine, J. *Adv. Phys. Org. Chem.* **1978**, *15*, 1–61. “The principle of least motion is the hypothesis that when multiple species with different nuclear structures could theoretically form as products of a given chemical reaction, the more likely to form tends to be the one requiring the least amount of change in nuclear structure or the smallest change in nuclear positions”.